Pergamon

PII S1359-6462(99)00152-9

VISCOELASTIC BEHAVIOR OF SUPERPLASTIC 37 wt% Pb 63 wt% Sn OVER A WIDE RANGE OF FREQUENCY AND TIME

P.M. Buechner[1], D. Stone[2] and R.S. Lakes[3]*

[1,3]Department of Engineering Physics
[1,3]Engineering Mechanics Program; [3]Biomedical Engineering Program
[3]Materials Science Program and [3]Rheology Research Center
[2]Department of Materials Science
University of Wisconsin-Madison
147 Engineering Research Building
1500 Engineering Drive, Madison, WI 53706-1687

Introduction

Viscoelasticity is manifested in transient experiments as creep or relaxation and in dynamic tests with sinusoidal loading, as a phase angle δ between stress and strain. Polymers (1) often exhibit large viscoelastic effects (the loss tangent, tan δ from 0.1 to 1 or more) at ambient temperature. In structural metals (2,3) such as steel, brass, and aluminum, viscoelastic effects are usually small (tan δ of 10^{-3} or less); some alloys exhibit a small tan $\delta < 10^{-5}$. Even so, all materials exhibit some viscoelastic response.

Some metals of low melting point exhibit relatively large creep and tan δ. For example, alloys of low melting point are often used as solders (4), and in these, creep can be problematical near room temperature since excessive flow and cracking can cause failure of an electronic device. Some metals, such as Cu-Mn (5) offer high damping in applications where polymer layers are inappropriate. A drawback of Cu-Mn is that it is nonlinear, and only achieves relatively high damping at high vibration amplitude. Alternative high-damping metals are therefore of interest.

Mechanical damping in metals is known to increase rapidly with temperature at homologous temperature $T_H > 0.5$, where $T_H = (T_{abs}/T_{melt}) \cdot T_{abs}$ is the absolute temperature and T_{melt} is the melting temperature (6). For structural metals such as steel, $T_H > 0.5$ corresponds to elevated temperature. For some elements (7) and low melting point alloys such as Pb-Sn and In-Sn, used as solders, room temperature is a high homologous temperature. In-Sn was also used, taking advantage of its high damping properties, tan δ greater than 0.1 below 0.1 Hz (8,9), to make a composite exhibiting high stiffness and high damping (10). Eutectic Pb-Sn, melts at 183 °C so $T_H \approx 0.65$ at room temperature,
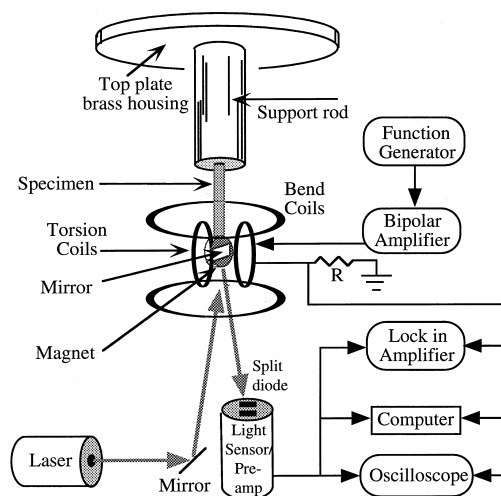
---

*Corresponding author.

Figure 1. Diagram of the broadband viscoelastic spectoscopy instrument.

22 °C. The purpose of the present study is to experimentally study the viscoelastic behavior of a superplastic Pb-Sn alloy over eleven decades of time and frequency using broadband viscoelastic spectroscopy. No appeal is made to time temperature superposition; all experiments were done at the same temperature.

Materials and Methods

Cast ingots of 37 wt% Pb-63 wt% Sn (and 44 ppm of metal impurities including 20 ppm Sb and 10 ppm Bi) were rolled at room temperature in increments of 10% permanent deformation in thickness for each pass down from 13.5 mm to 1.56 mm thickness, a total reduction of almost 90%. This treatment resulted in an average grain size (phase separation) of 4.5 μm in the longitudinal direction and 3.2 μm in the transverse direction.

Specimens were in the form of rectangular strips of dimensions 37 mm long and 1.56 mm thick. Three specimens of width 2.64, 2.46 and 2.28 mm were prepared using a low-speed diamond saw. Viscoelastic testing was performed using the modified (8,9) broadband viscoelastic spectroscopy apparatus (11) shown in Fig. 1. The instrument is capable of torsion and bending studies in creep, sub-resonant dynamic and resonant dynamic oscillation upon the same specimen. The wide frequency range capability of this apparatus is particularly useful in testing composites and other materials which are thermorheologically complex. Specimens were mounted using a cyanoacrylate cement, at the top to its support rod, at the bottom, to a high magnetic intensity neodymium iron boron magnet. Dynamic experiments were conducted by applying an amplified sinusoidal voltage from a digital function generator to the Helmholtz coil. This coil imposed a magnetic field on the permanent magnet and transmitted an axial torque on the specimen. The angular displacement of the specimen was measured using laser light reflected from a mirror mounted on the magnet to a split-diode light detector. The detector signal was amplified with a wideband differential amplifier. Torque was inferred from the Helmholtz coil current. Torque calculations were supported by calibrations using the well-characterized Al alloy type 6061-T6 (E = 68.9 GPa, G = 25.9 GPa, tan $\delta \approx 3.6 \times 10^{-6}$) (12). Input and output voltages were recorded using a digital data acquisition system containing a Macintosh IIci computer and LabVIEW[®] interface hardware and software. Quasistatic (creep) experiments were conducted by

applying a step function of current and monitoring both the current and the angular displacement signal as a function of time. Near resonances, signals were measured using a digitizing oscilloscope. At low frequency the phase angle between torque and angular displacement was determined from the width of elliptic Lissajous figures. At frequencies above 0.01 Hz, phase angle was determined using a lock-in amplifier (SRS 850) with claimed phase resolution 0.001 deg. The frequency range was segmented into regions less than 1 Hz and greater than 1 Hz since the wide frequency range necessitated different time constant settings. Tests were conducted 20 days, 41 days, and 77 days after rolling.

Data reduction was conducted using the relationship for the torsional rigidity (ratio of torque M^* to angular displacement θ) of a viscoelastic cylinder of radius R, length L, and density ρ with an attached mass of mass moment of inertia I_{at} at one end and fixed at the other end. For the present data of relatively low loss near the first resonance, it was sufficient to use a lumped approximation to obtain δ, the material phase angle in the subresonant region. For materials which have high loss δ near resonance, the exact relation is required (13). The lumped relations are as follows. $|G^*| = G'\sqrt{1 + \tan^2 \delta}$ and $\tan \delta = \tan \phi (1 - (\nu/\nu_o)^2)$. Here, ν_o is the natural frequency, ν is frequency and ϕ is the observed phase difference. G' is the storage shear modulus (a measure of stiffness), the real part of the complex dynamic modulus G^*. The loss tangent, $\tan \delta$, is a measure of mechanical damping. For frequency sufficiently below the first natural frequency, torsional stiffness is given by $|G^*| \approx K(|M^*|L)/\theta$, and loss by $\tan \delta \approx \tan \phi$ in which K is a geometrical factor for torsion of a rectangular section. For quasistatic bending, $|E^*| \approx 12|M^*|L/bh^3\theta$, with b and h as the rectangular cross section dimensions. At the resonance angular frequencies ω_o in torsion and bending, damping was calculated using the width $\Delta\omega$ at half maximum of the curve of dynamic structural compliance θ/M^* according to $\tan \delta \approx (1/\sqrt{3})$ $(\Delta\omega/\omega_o)$.

Each specimen was tested at a temperature of 22°C. In most experiments, input voltage (and thus shear stress) was held constant. The maximum surface strain at 1 Hz was 3.6×10^{-7} for torsion and 3.4×10^{-7} for bending. The initial peak strain was 0.95×10^{-7} for long term torsion creep, 1.1 to 4.9×10^{-7} for shorter term torsion creep, and 4.9×10^{-7} for bending creep. To distinguish linear from nonlinear behavior, the shape of the Lissajous figures was examined, and some tests were repeated at different strain levels.

Results and Discussion

Phenomena

The absolute value of the complex dynamic shear modulus G^* and the loss tangent $\tan \delta$ are plotted on a common scale along with the normalized inverse of the creep compliance J(t) (Figure 2). Computed errors are mostly comparable to or less than the size of the data points. Time t in creep is related to frequency ν in dynamic tests by $2\pi\nu = 1/t$. Tan δ in torsion followed a ν^{-n} dependence with n = 0.1988 over four decades from 0.01 to 100 Hz. This is in contrast to the ν^{-n} dependence over about seven decades of frequency for In-Sn examined earlier (9). The creep compliance showed no evidence of an asymptotic stiffness. The slope of the creep curve on a log-log scale progressively increased, reaching a value of m = 0.62 at the longest times. This is in contrast to the t^m creep behavior over more than four decades with m = 0.28 for In-Sn. Since m < 1, the strain rate is not constant so the creep is not secondary creep; it is still primary creep even at long times.

Tests of linearity disclosed tan δ at 1 Hz to be constant within experimental scatter for peak shear strains from 0.5 to 2.5×10^{-6}; damping increased by 5% at a strain of 3×10^{-6}. The shear modulus changed by about 1% over a strain range 10^{-7} to 2×10^{-6}. Lissajous figures were elliptical in shape indicating no obvious nonlinear effects.
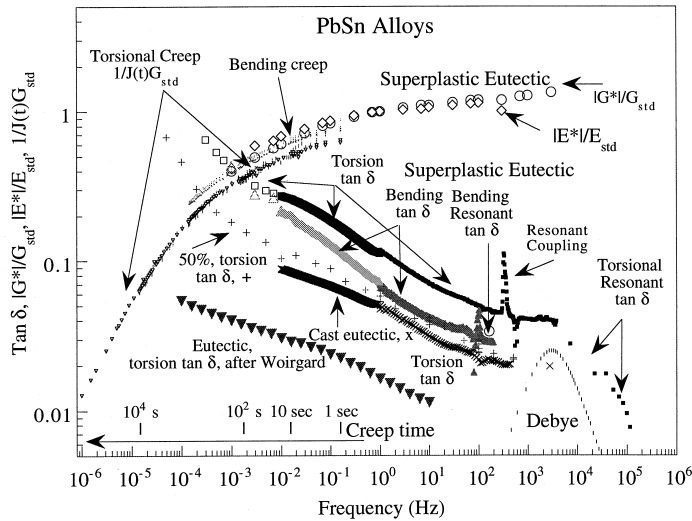
Figure 2. Viscoelastic properties of superplastic eutectic 37Pb-63Sn at 22 °C compared with those of eutectic 37Pb-63Sn (Woirgard et. al, 14), cast eutectic Pb-Sn and 50%Pb-Sn solder wire. Dynamic moduli $|G^*|$ and $|E^*|$ and creep compliances J(t) are normalized. The normalizing shear modulus is G_{std} (1 Hz) = 7.21 GPa. The normalizing Young's modulus is E_{std} (1 Hz) = 27.7 GPa. A theoretical Debye peak is shown for comparison.

There was no consistent aging effect in tan δ at 0.1 Hz from 20 days to 77 days after rolling; at 100 Hz, tan δ decreased by 3% from a baseline of 0.0495 from 20 days to 41 days, and by 11% from 20 days to 77 days after rolling. Cast alloy was aged five days.

As for instrumental effects, damping was reproducible within 0.5 to 5% of the total damping for the lock-in method, depending on settings, and within better than 15% of the total for the Lissajous method depending on settings. The spike in the torsion damping data near 300 Hz is due to a coupling with a bending mode; the spike in the bending data near 100 Hz is due to building vibration.

High levels of recoverable viscoelasticity (anelasticity) are known in fine-grained superplastic Sn-Pb alloys via transient recovery experiments (15). For comparison, tan δ was measured under sinusoidal excitation (16) from ambient temperature to near the melting point at four frequencies from 0.1 Hz to 0.4 Hz in uniaxial tension and compression. In the present bending results at 22 °C, tan δ ≈ 0.09 at 0.4 Hz, and in the results of Ref. (16), at 0.4 Hz at 34 °C, tan δ ≈ 0.11; if we extrapolate to 22 °C, tan δ ≈ 0.09, a satisfactory agreement. Torsional tan δ of superplastic Pb-Sn exceeded values for cast eutectic Pb-Sn by a factor of two to three, and also substantially exceeded values for eutectic Pb-Sn of (Woirgard et. al, 14) as shown in Fig. 2. The material studied by Woirgard was stated to be superplastic but no processing details were given.

Properties of superplastic Pb-Sn alloy are compared with other materials (17) in the stiffness-loss map in Fig. 3. The diagonal line in Fig. 3 presents the largest product (E tan δ ≈ 0.6 GPa) of stiffness E and damping, found in common materials, including polymers through the glass-rubber transition and soft metals such as Pb. Stiffness is considered as the absolute value of the complex dynamic Young's modulus $|E^*|$. It is possible to achieve higher E tan δ in composites designed to achieve such a figure of merit (for vibration absorption), as done by Brodt and Lakes (10), but such a combination is unusual in materials other than designed composites. Superplastic Pb-Sn alloy is seen to have an unusually high damping, even when compared with other metals of low melting point.
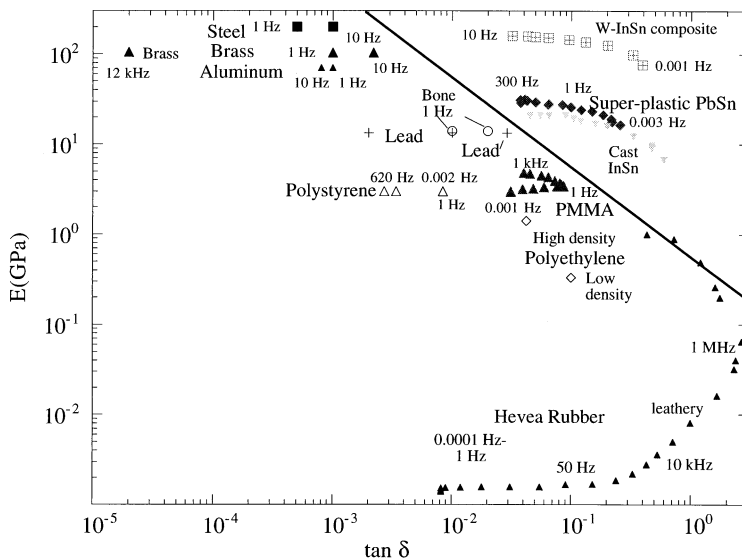
Figure 3. Stiffness-loss map comparing properties of Pb-Sn with those of other materials (9,10,17).

Mechanisms

Several mechanisms give rise to viscoelastic damping in metals at high homologous temperature (2,3). Since damping is over a broad band of frequency, mechanisms which predict a Debye peak are excluded in their pure form. However, such mechanisms may be considered provided that the time or length scale which governs the peak follows a broad distribution function.

For example, viscous slip at the grain boundaries as well as rearrangement of pairs of atoms in an alloy (Zener mechanism) give rise to peaks in tan δ which approximate the following Debye form, shown for comparison with experimental results in Fig. 2.

$$\tan \delta = \Delta \, \frac{\omega\tau}{1 + \omega^2\tau^2} \tag{1}$$

with τ as a relaxation time and $\omega = 2\pi\nu$, with ν as frequency and Δ as a constant. Such peaks cover about one decade of time or frequency. In Pb-Sn and In-Sn alloys at high homologous temperature, observed damping covers a much wider frequency range, therefore other mechanisms are to be considered.

Nowick and Berry (3) in their classic reference on anelastic behavior observed that the high temperature background has magnitude which is smaller in single crystals than in polycrystals; it is smaller in coarse-grained polycrystals than in fine-grained polycrystals; and it is enhanced in deformed and partially recovered samples. High temperature background is thought to be caused by a combination of thermally activated dislocation mechanisms (18). Assuming a generic thermally activated disloca-tion-point-defect mechanism (18); for a distribution of activation energies and negligible restoring force on the dislocations gave rise to the following form which follows a power law in frequency.

$$\tan \delta = \frac{Q}{[2\pi\nu \, \exp \, (U_0/kT_{abs})]^n} \tag{2}$$

where U_0 is the activation energy of the rate-controlling process, ν is frequency, T_{abs} is the absolute temperature, and Q and n are constants. This relaxation process is, however, not well enough understood to permit prediction of the magnitude of the viscoelastic response of a given pure metal or alloy.

The damping in torsion is higher than in bending; the difference is more marked at high frequency. As for low frequency and creep, torsion and bending results are similar. Since the grains are elongated in the specimen axis direction, torsion load gives rise to shear stress across the boundaries, while bending stress does not. The values of shear modulus and Young's modulus observed here imply anisotropy: Young's modulus E is too large in relation to the shear modulus for the isotropic relationship between them to be satisfied. Anisotropy is consistent with the elongated grain structure. The results suggest a role for the boundaries. In that vein, several boundary mechanisms were considered in Ref. (15). Grain boundary slip following Zener was considered insufficient to explain the large relaxation strengths observed. Grain shape changes that accompany sliding were also considered as a mechanism. These changes could lead to an anelastic effect due to increase in boundary area per unit volume accompanying shape change. Other grain boundary effects were considered unlikely in view of the wide spectrum of relaxation times observed. Models based on voids and dislocation pile-up were considered as possibilities (15). It is recognized that superplasticity in the fine-grained Pb-Sn eutectic is caused by inter-phase boundary sliding. The superplastic properties are known to be a strong function of grain size. Such sliding might be in part responsible for the enhanced tan δ in this alloy as well. However cast In-Sn exhibits tan $\delta \propto \nu^{-n}$ over many decades without any multiplication of grain boundaries. By appeal to Occam's razor, dislocations are likely to be more important in superplastic Pb-Sn as well.

Conclusions

Damping of superplastic eutectic Pb-Sn is considerably higher than that of cast Pb-Sn, solder wire, and eutectic Pb-Sn reported by Woirgard et al. Tan δ approximately follows a ν^{-n} dependence over about four decades of frequency. The damping in torsion is higher than in bending; the difference is more marked at high frequency.

Acknowledgments

References

1. J. D. Ferry, Viscoelastic Properties of Polymers, 2nd edn., John Wiley, New York (1979).
2. C. Zener, Elasticity and Anelasticity of Metals, University of Chicago Press, Chicago (1948).
3. A. S. Nowick and B. S. Berry, Anelastic Relaxation in Crystalline Solids, p. 435, Academic Press, New York (1972).
4. J. S. Hwang, in Electronic Packaging and Interconnection Handbook, ed. C. A. Harper, McGraw-Hill, New York (1991).
5. I. G. Ritchie, K. W. Sprungmann, and M. Sahoo, J. Phys. 46, C10–409 (1985).
6. T. S. Kê, J. Appl. Phys. 21, 414 (1950).
7. L. S. Cook and R. S. Lakes, Scripta Metall. Mater. 32, 773 (1995).
8. M. Brodt, L. S. Cook, and R. S. Lakes, Rev. Sci. Instrum. 66, 5292 (1995).
9. R. S. Lakes and J. Quackenbush, Phil. Mag. Lett. 74, 227 (1996).
10. M. Brodt and R. S. Lakes, J. Composite Mater. 29, 1823 (1995).
11. C. P. Chen and R. S. Lakes, J. Rheol. 33, 1231 (1989).
12. W. Duffy, J. Appl. Phys. 68, 5601 (1990).
13. W. G. Gottenberg and R. M. Christensen, Int. J. Eng. Sci. 2, 45 (1964).

14.   J. Woirgard, Y. Sarrazin, and H. Chaumet, Rev. Sci. Instr. 48, 1322 (1977).
15.   J. H. Schneibel and P. M. Hazzledine, Acta Metall. 30, 1223 (1982).
16.   B. Baudelet and C. Homer, Scripta Metall. 11, 185 (1977).
17.   R. S. Lakes, Viscoelastic Solids, CRC Press, Boca Raton, FL (1998).
18.   G. Schoeck, E. Bisogni, and J. Shyne, Acta Metall. 12, 1466 (1964).